Is the Lack of Pulsations in Low Mass X-Ray Binaries due to Comptonizing Coronae?

Ersin Göğüş[1], M. Ali Alpar[1], Marat Gilfanov[2,3]

ABSTRACT

The spin periods of the neutron stars in most Low Mass X-ray Binary (LMXB) systems still remain undetected. One of the models to explain the absence of coherent pulsations has been the suppression of the beamed signal by Compton scattering of X-ray photons by electrons in a surrounding corona. We point out that simultaneously with wiping out the pulsation signal, such a corona will upscatter (pulsating or not) X-ray emission originating at and/or near the surface of the neutron star leading to appearance of a hard tail of Comptonized radiation in the source spectrum. We analyze the hard X-ray spectra of a selected set of LMXBs and demonstrate that the optical depth of the corona is not likely to be large enough to cause the pulsations to disappear.

Subject headings: accretion, neutron star physics – X-rays: Binaries – stars: individual (GX 9+1), (GX 9+9), (Sco X-1)

1. Introduction

Low mass X-ray binaries (LMXBs) are binary systems that contain a neutron star or a black hole as the primary object, and a low-mass star (typically $M < 2\ M_{Sun}$) as the mass-donating companion. Mass transfer from the companion takes place via Roche lobe overflow.

In the case of neutron star LMXBs, the neutron star spin period would be expected to be observable if the magnetic fields of the star can channel the accretion to yield beamed X-ray emission, and if the beamed signal can escape the system. The fact that almost none of the LMXBs exhibit pulsations corresponding to the neutron star spin period has remained a puzzle since the discovery of neutron star LMXBs. The proposal that the millisecond radio pulsars are evolutionary descendants of the low mass X-ray binaries (Alpar et al. 1982; Radhakrishnan & Srinivasan, 1983) highlighted the issue

[1]Sabancı University, Faculty of Engineering & Natural Sciences, Orhanlı−Tuzla 34956 İstanbul, Turkey

[2]Max-Planck-Institute für Astrophysik, Karl-Schwarzschild-Str. 1, 85740 Garching bei München, Germany

[3]Space Research Institute, Russian Academy of Sciences, Profsoyuznaya 84/32, 117997 Moscow, Russia

and led to a search for millisecond X-ray pulsars. Millisecond spin periods were also indicated in the initial beat frequency model for horizontal branch quasi periodic luminosity oscillations (Alpar & Shaham 1985). More recently, kilohertz QPO branches also gave an indication of millisecond rotation periods through a beat frequency model interpretation of the difference between two "kilohertz" frequency bands. The burst oscillations observed from these sources seem to have about the difference frequency or half the difference frequency. While a consistent interpretation of kilohertz, burst and horizontal branch oscillations is not available yet, there are enough correlations and systematics (van der Klis 2000) at high frequency bands that, assuming the accretion flow and the neutron star are not far from rotational equilibrium, all these high frequency QPO observations also point at rapid neutron star spin, with periods in the millisecond range.

Millisecond X-ray pulsars were discovered relatively recently (Wijnands & van der Klis 1998), confirming the evolutionary hypothesis. These millisecond X-ray pulsars (or, indeed , pulsars of any coherent spin period) remain a minority among the LMXBs. Almost 90% of LMXBs do not display coherent pulsations in their persistent phase. So the question remains as to why these few among the LMXBs display their spin period.

The millisecond radio pulsars are believed to have spun up to these exremely short spin periods by accretion. To have millisecond equilibrium periods at sub-Eddington accretion rates the magnetic field strength of the compact object should be relatively weak ($B \sim 10^9$ G). Nevertheless, a magnetic field of this magnitude may be able to channel the accretion flow and lead to beamed X-ray radiation. The inner radius of the accretion disk, roughly the Alfven radius, is expected to be a few stellar radii in most LMXBs. This leaves a possibility of a magnetosphere with ample options for anisotropy in accretion and beaming for the X-ray radiation.

The absence of coherent pulsations in the persistent emission of neutron star LMXBs is usually attributed to several potential causes as laid out already in the first papers on the evolution of millisecond radio pulsars (Alpar et al. 1982, Alpar and Shaham 1985, Lamb et al 1985): *(i)* The magnetic field is so weak that accreting matter cannot be channeled onto the magnetic poles, *(ii)* The pulsar's periodic signal is attenuated by gravitational lensing (e.g. Meszaros, Riffert & Berthiaume 1988), *(iii)* Beamed radiation emerging from the neutron star's magnetic polar caps is "wiped out" by electron scattering (Brainerd & Lamb 1987; Kylafis & Klimis 1987; Wang & Schlickeiser 1987; Bussard et al. 1988). It is important to note the distinction between isotropic luminosity oscillations and modulation in the observed signal due to a rotating beam. Although in both cases scatterings will suppress pulsations as observed by a distant observer, the physics of suppression is different (e.g. Miller, Lamb, & Psaltis 1998). In the case of isotropic luminosity oscillations, the degree of suppression of pulsations depends on the ratio of the light travel time in the scattering media (which depends on its optical depth and size) to the pulsation period. In the case

of modulations due to rotating beamed radiation, the optical depth of ~ 1 is sufficient to destroy the beaming and to wipe out pulsations. While the luminosity oscillation may be relevant to QPO phenomena in X-ray binaries, it is the beaming oscillations, that are responsible for coherent pulsations observed from X-ray pulsars. The latter case is critically investigated in the paper.

In the commonly accepted picture of sub-Eddington accretion onto a neutron star, two parts of the accretion flow are distinguished - the Keplerian accretion disk and the boundary/spreading layer on the surface of the neutron star (Sunyaev & Shakura 1986). The boundary/spreading layer is present in neutron stars with magnetic field not strong enough to stop the acretion disk beyond a magnetosphere. In the boundary/spreading layer the accreting matter decelerates from the Keplerian velocity of the inner boundary of the accretion disk to the rotation velocity of the neutron star and settles onto its surface. Comparable fractions of energy are emitted in the disk and in the boundary layer (Sibgatullin & Sunyaev 2000). Correspondingly, there are two components in the spectra of neutron star binaries, associated with these two parts of the accretion flow. At sufficiently high mass accretion rate $\dot{M} > 0.1\ \dot{M}_{\rm Edd}$, corresponding to the high spectral state of atoll and Z-sources, the boundary layer and accretion disk are both radiating in the optically thick regime with kT$\sim$1$-$2 keV. It is expected on theoretical grounds and demonstrated observationally that the boundary layer component has higher temperature than the accretion disk (Gilfanov, Revnivtsev & Molkov 2003).

A corona around the neutron star, responsible for wiping out the pulsating signal will upscatter the relatively soft emission from the neutron star surface (pulsating or not). Depending on the geometry, some fraction of the accretion disk emission will also be upscattered. This will lead to appearance of the hard tail of Comptonized emission in the spectrum. Transient hard tails are indeed observed in the spectra of neutron star LMXBs and are sometimes attributed to the Comptonization (see e.g., Di Salvo et al. [2000]). However, these hard tails are not always present.

Hard X-ray upper limits (or detected flux) can be used to constrain parameters of the putative corona around the neutron stars. Indeed, if the spectrum and intensity of the neutron star surface emission are given, the flux in a high energy band (e.g. 30$-$60 keV) will depend uniquely on the temperature and optical depth of the corona. The critical parameter in the "wiping out" scenario is, of course, the optical depth. One can consider a range of plausible temperatures and constrain the optical depth of the corona as a function of its (unknown) temperature. If, on the other hand, the hard tail is significantly detected, the position of its high energy cutoff can help to determine the temperature and more accurately constrain the optical depth.

In this study, we perform broadband X-ray spectral investigations of the three LMXBs, GX 9+1, GX 9+9 and Sco X-1 to constrain their hard X-ray spectral characteristics using a Comptonization model. We estimate the spectrum and flux of the

seed photons for Comptonization (i.e. neutron star surface spectrum) by applying a two-temperature black body model to the observed spectrum below ∼20 keV. In this simplified model, the harder blackbody represents emission of the surface of the neutron star (boundary/spreading layer). The softer blackbody is a crude approximation to the emission of the accretion disk, ignoring the temperature distribution in the disk and the effect of scatterings. The Comptonization model is mainly characterized with the usual two parameters, the electron scattering optical thickness τ and the electron temperature kT_e. Values of $\tau \gtrsim 1$ would destroy the beamed radiation from the surface of the neutron star. We can, therefore, check the validity of the electron scattering scenario for the absence of coherent pulsations from these systems by using the upper limits to hard X−ray emission to obtain upper limits of τ for a range of electron temperatures and conclude whether or not the optical depth of a corona is large enough to smear out the beamed radiation from the neutron star. In the following section we describe the data used in this study. We present our spectral investigations in §3. The results are presented in §4, discussion and conclusions in §5.

2. Observations and Data Extraction

We used archival Rossi X−ray Timing Explorer (RXTE) pointing observations of GX 9+1, GX 9+9 and Sco X−1. These sources are selected to reflect broad characteristics of LMXBs. GX 9+1 and GX 9+9 are known as atoll sources and their X-ray intensities are in the range of low (0.1 L_{Edd}) to intermediate (0.4 L_{Edd}) levels. Sco X-1 is a Z source which is the brightest X-ray emitting system among LMXBs ($\gtrsim L_{Edd}$). In Table 1 we list the details of the RXTE pointed observations.

RXTE consists of two main instruments. The Proportional Counter Array (PCA) is an array of five nearly identical xenon Proportional Counter Units (PCUs), which are sensitive to photon energies between 2−60 keV. Each detector unit has a collecting area of 1300 cm^2 and energy resolution of 18% at 6 keV (Jahoda et al. 2006). The High-Energy X-Ray Timing Experiment (HEXTE) consists of two clusters of NaI/CsI scintillation detectors which are sensitive to photons of energies between 15 and 250 keV. The energy resolution of HEXTE detectors is 15% at 60 keV (Rothschild et al. 1998).

We extracted the PCA spectra using Standard2 data (129 channels accumulated every 16 s) collected from all three layers of all five PCUs. In selecting data we required the Earth elevation angle with respect to the spacecraft to be greater than 10° and the time to the nearest South Atlantic Anomaly passage to be more than 30 minutes. A background spectrum was generated using the bright source background models, provided by the PCA instrument team and pcabackest, which is an

Table 1: Log of RXTE observations.

Source	ObsID	Date	Exp (ks)
GX9 + 1	20064-01-01-00	10/02/1997	11.8
GX9 + 9	10072-04-02-00	16/10/1996	10.1
ScoX − 1	20053-01-01-05	23/04/1997	15.1

HEASOFT utility. The detector dead time correction was applied for both the PCA and HEXTE spectra due to very bright X-ray output of the sources selected. We performed X-ray spectral modeling using XSPEC version 11.3.1 (Arnaud 1996). We added a 1% systematic error to the statistical error of each PCA spectral channel to account for the detector response uncertainties.

3. Spectral Analysis

We initially modeled the PCA spectrum only (in 3−20 keV) to determine the spectral characteristics of these sources at low X-ray energies. The hydrogen column densities (N_H) were fixed at the interstellar average values in the direction of each source (Dickey & Lockman, 1990). The interstellar N_H values are 9×10^{21} cm^{-2}, 2×10^{21} cm^{-2}, and 1.5×10^{21} cm^{-2} for GX 9+1, GX 9+9, and Sco X-1, respectively.

The X-ray spectrum of GX 9+1 is well fit with a sum of two blackbody functions. The blackbody temperatures are 1.96±0.02 keV and 1.08±0.02 keV. The emission radius of the higher temperature blackbody is 7.8±0.4 km, while the radius of the lower temperature blackbody is 22.8±0.7 km (assuming a distance of 10 kpc). We take the former blackbody component as the emission originating from nearby the neutron star surface. Note that these radii may not represent exact emission areas due to effect of scattering and orbital inclination. The unabsorbed 2−20 keV flux values of the blackbody components are 9.14×10^{-9} erg cm^{-2} s^{-1} and 6.46×10^{-9} erg cm^{-2} s^{-1}, respectively.

In case of GX 9+9 spectral fitting, a broad spectral line was required to adequately fit the spectrum, as well as two blackbodies. The blackbody temperatures are 2.02±0.06 keV and 0.88±0.02 keV, and the radii of corresponding emitting regions are 3.9±0.2 km and 21.6±0.9 km (assuming a source distance of 10 kpc). The centroid energy of the broad line feature was fixed at 6.4 keV (that is, the rest frame energy of cold iron). We found a line width of 1.05±0.03 keV and the equivalent width of 240±22 eV. Similar to the case in GX 9+1, we take the 2.02 keV blackbody as emitting from on or near the neutron star surface. We estimate the unabsorbed 2−20 keV flux values as 2.65×10^{-9} erg cm^{-2} s^{-1} and 1.96×10^{-9} erg cm^{-2} s^{-1} for the harder and softer blackbody components, respectively.

As for Sco X-1, the sum of two blackbody components and a broad line feature yields a suitable fit to the X-ray spectrum. The blackbody temperatures are 2.27±0.01 keV and 0.78±0.01 keV. The radii of emitting regions are 5.3±0.3 km and 54.1±1.5 km (using the distance estimate of 2.8 kpc [Bradshaw, Fomalont & Geldzahler 1999]). The width of the line feature (the centroid fixed at 6.4 keV) is 1.15±0.1 keV and the equivalent width is 848±9 eV. The unabsorbed fluxes in the 2−20 keV range are estimated as 1.13×10^{-7} erg cm^{-2} s^{-1} and 1.05×10^{-7} erg cm^{-2} s^{-1} for the harder and softer blackbody components, respectively.

For each source, we then modeled the PCA (3−20 keV) and HEXTE (15−200 keV) spectra simultaneously as follows. We fixed the spectral parameters of the low energy portion on their above determined values and added an extra Comptonized component (COMPPS model in XSPEC,

spherical geometry [Poutanen & Svensson 1996]). The spectrum and normalization of the seed photons for the Comptonization were fixed at the parameters of the harder black body component, representing the emission originating on or near the surface of the neutron star. The only two remaining parameters of the Comptonization model are the electron temperature, kT_e and optical depth, τ in the Comptonization region. For a given value of the temperature, the upper limit on the optical depth can be computed such that the upper limits on the hard X-ray flux (30−200 keV) are satisfied. Thus temperature dependent optical depth upper limits can be obtained in the temperature range of interest.

In Figure 1 we present the observed broadband X-ray spectrum of GX 9+1 with the sum of two blackbody components (solid line) and 2σ upper limits to the hard X-ray emission. Also in Figure 1, we illustrate some representative Comptonization spectra (obtained using COMPPS). While performing the simultaneous fit, we fixed the electron temperature of the Comptonizing cloud (kT_e) at 11 preselected values ranging from 10 to 100 keV and increasing by an increment of 10 keV, with an additional upper limit at kT_e=15 keV to better understand the trend at low electron temperatures. We determined the upper limits for the electron scattering optical depths (τ) of the assumed Comptonizing corona at 95% confidence level.

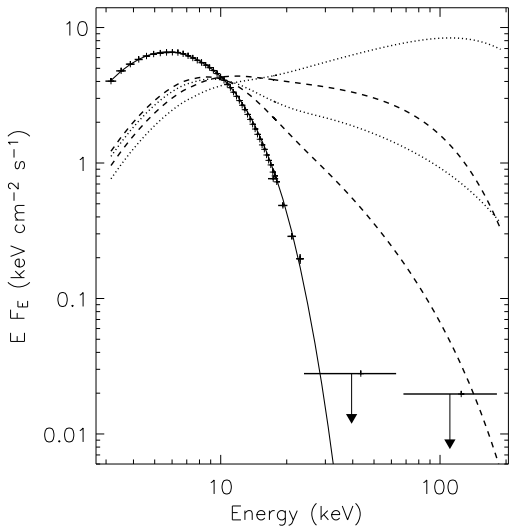

Fig. 1.— The broadband X-ray spectrum of GX 9+1 as seen with the RXTE/PCA and HEXTE. The upper limits at high energies are at 2σ level. The solid curves are the two blackbodies that fit the PCA spectrum. The illustrative Comptonization curves obtained with the electron cloud temperatures, kT_e=30 keV (dashed) and kT_e=60 keV (dotted), both using τ=1 (lower curves) and τ=3 (upper curves). The higher temperature black body component, representing the neutron star surface emission was used as the seed for Comptonization.

4. Results

We present the 2σ upper limit values for Compton scattering optical depth (τ) as a function of selected temperatures of scat-

tering electron cloud (kT_e) of GX 9+1 in Figure 2. We estimate the electron scattering optical depth, $\tau \sim 0.23$ even at the lowest scattering corona temperature considered (i.e., $kT_e = 10$ keV). At higher electron temperatures the upper limit to the optical depth rapidly decreases. This strongly indicates that for GX 9+1 the assumed corona is not optically thick enough to significantly alter the nature of seed photons originating from near the stellar surface via Compton scattering.

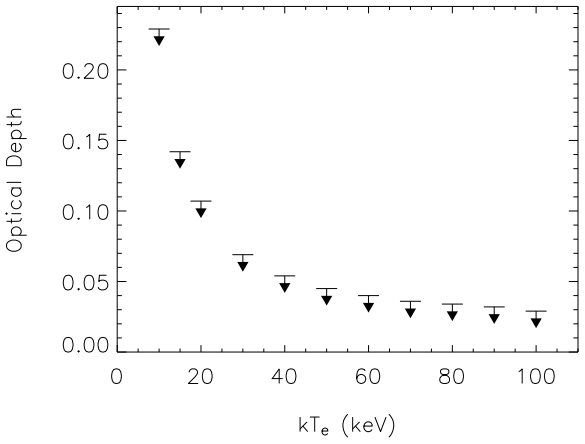

Fig. 2.— Plot of the estimated 2σ upper limits for the optical depth as a function of the temperature of the electron cloud in GX 9+1.

As an independent check, we have followed the same line of analysis but used a different RXTE pointing observation of GX 9+1 (Observation ID: 30042-05-02-00 performed on 27 September 1998 with an exposure time of ∼7.4 ks). We obtain a similar $kT_e - \tau$ trend as seen in Figure 2.

In Figure 3, we show the optical depth upper limits as a function of assumed kT_e around GX 9+9. We find that the upper limits to the scattering optical depth in this source are higher compared to that in GX9+1 at the lowest assumed electron corona temperature. Similar to the case in GX 9+1, the upper limits to the optical depth fall down rapidly as the assumed electron cloud temperature increases. We find that the optical depth of the assumed corona around GX 9+9 does not seem to be sufficient to suppress any beaming present in the incoming soft X-ray radiation.

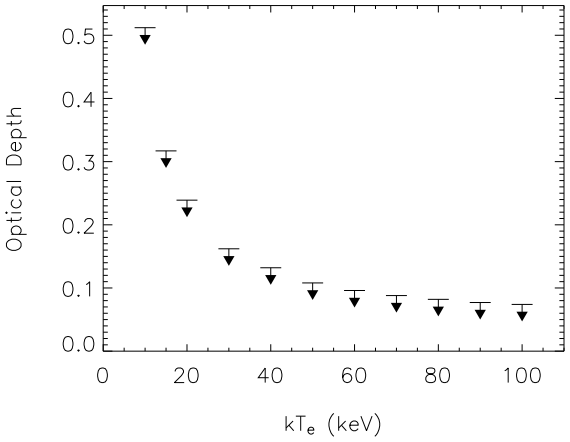

Fig. 3.— Plot of the estimated 2σ upper limits for the optical depth as a function of the temperature of the electron cloud in GX 9+9.

Finally in Figure 4, we present the upper limits to τ as a function of kT_e in Sco X-1. The overall trend is very similar to those in both aforementioned sources. It is noteworthy here that the 2σ upper limit to the optical depth for the lowest electron cloud temperature of 10 keV is almost 1.1. Such a degree of optical thickness may cause a significant change on the properties of the incident radiation. Nevertheless, at electron cloud temperatures $kT_e \gtrsim 15$ keV

the scattering optical depth upper limits drops down to about 0.6. Thus, a possible corona around Sco X-1, if it permanently exists, is not optically thick enough for electron scattering to efficiently play an important role in changing the beaming of soft X-rays emitted near the neutron star, unless the electron temperature is less than $\sim$10$-$15 keV.

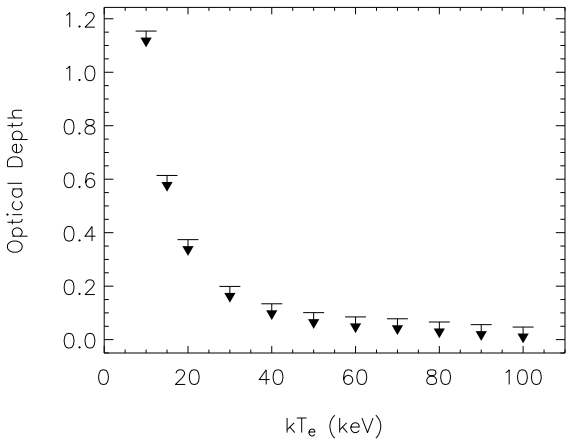

Fig. 4.— Plot of the estimated 2σ upper limits for the optical depth as a function of the temperature of the electron cloud in Sco X-1.

As in the case of GX 9+1, we performed the optical depth estimation procedure using another RXTE observation of Sco X-1 as well. (Observation ID: 10061-01-03-00 performed on 2 January 1998 for $\sim$5.5 ks). We find that the 2σ upper limit to the optical depth corresponding to a kT_e of 10 keV as 0.96 and τ values follow a similar trend for kT_e as was the case in Figure 4.

5. Discussion and Conclusions

5.1. Other LMXBs

Among the LMXBs there are six Z sources, including Sco X-1, which have hard X-ray tails in their spectra, though only episodically (GX 5-1: Asai et al. 1994, Paizis et al. 2005; Cyg X-2: Frontera et al. 1998; Di Salvo et al. 2002; GX 17+2: Di Salvo et al. 2000, Farinelli et al. 2005; Sco X-1: D'Amico et al. 2001; GX 349+2: Di Salvo et al. 2001; Cir X-1: Iaria et al. 2001). In all these reported hard tail cases, the hard X-ray spectral component is modelled with a power law (i.e., F(E) $\propto E^{-\gamma}$ whose index ranges between -1 and 3.3. The transient appearance of the hard X-ray tail in these sources is not correlated with the position of the source radiation properties in the color-color diagram (except for GX 17+2, Di Salvo et al. 2000, but also see Farinelli et al. 2005).

For Sco X-1, the episodic hard X-ray spectral tail was detected only in 5 RXTE pointings and the spectra were fitted with a power law of indices ranging from -0.7$\pm$0.7 to 2.4$\pm$0.3 (D'Amico et al. 2001). The 30$-$200 keV fluxes of these 5 observations range between 8.9×10^{-10} and 2.1×10^{-9} erg cm^{-2} s^{-1}, while we estimate the 30$-$200 keV flux for the RXTE pointing we investigate here as 4.2×10^{-10} erg cm^{-2} s^{-1}. If there indeed exists a Compton scattering cloud around the neutron star and it is the cause of the episodic hard X-ray emission, then it may be a possible scenario for suppressing the beaming and pulsed signals. However, such an explanation would work only during the epochs with hard tails. For the rest of the time there are only upper limits for

the optical depth, which are far below the regime of efficient scattering, indicating that the scattering corona is not likely to be thick enough to yield the suppression of the pulses. One is then left still needing a reason other than Comptonization to explain why coherent pulses are not observed.

5.2. Comptonization Models for the Accreting Millisecond Pulsars

There are now seven known millisecond X-ray pulsars. All of them have spectra with hard X-ray components which are fit well with Comptonization models. For the source XTE J1751-305, Gierlinski and Poutanen (2005) employ seed photons at the temperature ∼0.5 keV of the soft blackbody spectral component observed. With the COMPPS model of Comptonization they find kT_e = 29±4 keV and τ = 1.93±0.23. If the seed photon temperature is treated as a free parameter, the COMPPS model gives kT_e = 36±3 keV and τ = 1.47±0.26. The other Comptonization models tried by Gierlinski and Poutanen (2005) do not constrain the optical depth τ and yield electron temperatures in the range 22-42 keV. For SAX 1808.4−3658, application of the COMPPS model with seed photon temperature ∼0.65 keV from the soft blackbody spectral component gives kT_e = 43±9 keV and τ = 2.7±0.4 (Gierlinski, Done and Barret 2002). They have also found that the Comptonized spectral component does itself pulsate. For XTE J1807−294, Falanga et al. (2005a) performed a broadband spectral analysis using XMM-Newton, RXTE and INTEGRAL observations. They find $kT_e = 37^{+28}_{-10}$ keV and $\tau = 1.7^{+0.5}_{-0.8}$ using COMPPS with seed photon temperature of 0.75 keV. The hard X-ray spectrum of IGR J00291+5934 was adequately modelled with a different Comptonization model (COMPST, Sunyaev & Titarchuk 1980) and it was found that $kT_e = 25^{+21}_{-7}$ keV and $\tau = 3.6^{+1.0}_{-1.3}$ (Shaw et al. 2005). Falanga et al. (2005b) found significant pulsations up to ∼150 keV in IGR J00291+5934, indicating phase variations of the Comptonized component. Therefore, the geometry of the Comptonizing region in these sources could be different than that in non-pulsing neutron star LMXBs

Krauss & Chakrabarty (2006) have carried out a systematic X-ray spectral analysis of RXTE data of three millisecond X-ray pulsars and three sources that display no pulsations but burst oscillations. They have modeled the PCA and HEXTE spectra using absorbed blackbody plus Comptonization (COMPTT in XSPEC, Titarchuk [1994]) models. They find optical depths in the range of 2−5 and plasma temperatures ranging from ∼20 keV to 50 keV. They find no distinguishing spectral properties between the coherently pulsing and non-pulsing sources. Moreover, they also find degeneracy between the estimated optical depths and plasma temperatures. Based on these issues, they question the validity of the scattering scenario for the lack of pulsations.

5.3. Conclusions

We revisit the Compton scattering scenario suggested earlier to explain lack of pulsations in the majority of LMXBs. We point out that simultaneously wiping out the pulsating signal, such a corona would

upscatter X-rays orginating from the neutron star surface leading to appearance of a hard tail of Comptonized radiation in the source spectrum. We utilize archival data of RXTE observations of 3 representative LMXBs (GX9+9, GX9+1 and Sco X-1) covering the full range of atoll/Z phenomenology. Based on the upper limits on the hard X-ray emission in the 30-200 keV energy domain and a simple but robust method to determine the neutron star surface emission we demonstrate that the optical depth of such a corona does not exceed $\tau \lesssim 0.2-0.5$, unless the electron temperature is very low, $kT_e \lesssim 20-30$ keV. Such small values of the optical depth are by far insufficient to suppress the pulsations. We therefore conclude that lack of coherent pulsations can not be attributed to the electron scatterings in the corona, at least in the present three sources, and possibly in other LMXBs to the extent that these sources are typical. A more likely cause of the lack of pulsations is the absence or weakness of beaming of the X-ray radiation emerging from the neutron star surface, caused, for example, by the weakness of the magnetic field in high $\dot{M}$ sources. In addition, the bending of X-rays in the gravitational field of the compact object may play some role (Meszaros, Riffert & Berthiaume 1988, Özel 2007, in preparation). Regarding the accreting millisecond X-ray pulsars, which exhibit pulsations in spite of evidence for Comptonization with $\tau > 1$, we note that the geometry of the Comptonization region must be different in these sources, e.g., localized near the neutron star polar cap, as suggested by the fact that the Comptonized spectral component in these sources itself pulsates.

We thank Feryal Özel and Dimitrios Psaltis for helpful discussions, and Rudy Wijnands for providing the database of accreting millisecond X-ray pulsars. M.A.A. and E.G. acknowledge partial support from the Turkish Academy of Sciences, for E.G. through grant E.G/TÜBA−GEBİP/2004−11.

REFERENCES

Alpar, M. A., Cheng, A. F., Ruderman, M. A. & Shaham, J. 1982, Nature, 300, 728

Alpar, M. A. & Shaham, J. 1985, Nature, 316, 239

Arnaud, K.A., 1996, ADASS V, eds. Jacoby G. & Barnes J., p17, ASP Conf. Series, 101

Asai, K., Dotani, T., Mitsuda, K., et al. 1994, PASJ, 46, 479

Barret, D. & Olive, J. F. 2002, ApJ, 576, 391

Bradshaw, C. F., Fomalont, E. B., & Geldzahler, B. J. 1999, ApJ, 512, L121

Brainerd, J. & Lamb, F. K., 1987, ApJ, 317, 33

Bussard, R. W., Weisskopf, M. C., Elsner, R. F., & Shibazaki, N. 1988, ApJ, 327, 284

D'Amico, F., Heindl, W. A., Rothschild, R. E. & Gruber, D. E. 2001, ApJ, 547, L147

Dickey & Lockman, 1990, ARAA. 28, 215

Di Salvo, T., Stella, L., Robba, N. R., et al. 2000, ApJ, 544, L119

Di Salvo, T., Robba, N. R., Iaria, R., et al. 2001, ApJ, 554, 49

Di Salvo, T., Farinelli, R., Burderi, L., et al. 2002, A & A, 386, 535

Falanga, M. et al. 2005, A & A, 436, 647

Farinelli, R. et al. 2005, A & A, 434, 25

Frontera, F. et al. 1998, The Active X-ray Sky, eds. L. Scarsi, H. Bradt, P. Giommi, & F. Fiore, Nuclear Physics, Proc. Suppl. 69/1-3, 286

Gierlinski, M. & Done, C. 2002, MNRAS, 331, 47

Gierlinski, M., Done, C., & Barret, D. 2002, MNRAS, 331, 141

Gierlinski, M. & Poutanen, J. 2005, MNRAS, 359, 1261

Gilfanov, M., Revnivtsev, M. & Molkov, S. 2003, A&A, 410,217

Jahoda, K. et al. 2006, ApJS, 163, 401

Kylafis, N. D. & Klimis, G. S., 1987, ApJ, 323, 678

Krauss, M. I. & Chakrabarty, D., 2006, In proc. of "A life with stars", eds. L. Kaper, M. van der Klis, and R. Wijers, Elsevier

Lamb, F. K., Shibazaki, N., Alpar, M. A., & Shaham, J. 1985, Nature, 317, 681

Maccarone, T. J. & Coppi, P. S. 2003, A & A, 399, 1151

Meszaros, P., Riffert, H., & Berthiaume, G. 1988, ApJ, 325, 204

Miller, M.C., Lamb, F.K. & Psaltis, D. 1998, ApJ, 508, 791

Paizis, A. et al. 2005, A & A, 444, 357

Poutanen, J. & Svensson, R. 1996, ApJ, 470, 249

Radhakrishnan, V. & Srinivasan, G. 1982, Current Science, 51, 1096

Rothschild, R. E. et al. 1998, ApJ, 496, 538

Shaw et al. 2005 A & A 432, L13

Sibgatullin, N. R. & Sunyaev, R. A. 2000, Astronomy Letters, 26, 699

Sunyaev, R. A., & Titarchuk, L. G. 1980, A & A, 86, 121

Sunyaev, R. A., & Shakura, N.I. 1986, SvAL, 12, 117

Titarchuk, L. 1994, ApJ, 434, 570

Van der Klis, M. 2000, ARA & A, 38, 717

Wang, Y. M. & Schlickeiser, R. 1987, ApJ, 313, 200

Wijnands, R. & van der Klis, M. 1998, Nature, 394, 344

This 2-column preprint was prepared with the AAS LaTeX macros v5.2.